International Journal of Environmental Science and Technology (2026) 23:578
https://doi.org/10.1007/s13762-026-07371-2

ORIGINAL PAPER

Sustainable electrocoagulation treatment of tetracycline contaminated water: coupling response surface methodology with life cycle assessment

S. Mirkhalafi[1,2] · M. Kiehbadroudinezhad[3] · H. Hosseinzadeh-Bandbafha[4] · M. Mousazadehgavan[1] · K. S. Hashim[1,5,6]

Received: 11 March 2026 / Revised: 1 June 2026 / Accepted: 9 July 2026 / Published online: 19 August 2026

Abstract

Tetracycline (TC), widely used in medicine and agriculture, has emerged as a persistent micropollutant in aquatic environments, posing significant risks to human health and ecosystems due to its environmental persistence and the inefficiency of conventional treatment methods. This study aimed to develop an efficient and sustainable electrocoagulation (EC) process using aluminum electrodes to remove TC from aqueous solutions. A Box–Behnken Design (BBD) combined with Response Surface Methodology (RSM) was employed to optimize four key operational parameters, including initial pH, current intensity, inter-electrode distance, and electrolysis time. To evaluate broader sustainability, life cycle assessment (LCA) and operational cost analysis were integrated into the methodology to quantify environmental impacts and economic feasibility under optimized conditions. The developed quadratic model showed good agreement between predicted and experimental results ($R^2 = 0.887$), confirming the reliability of the optimization approach. TC removal efficiencies reached up to 100% under optimized operating conditions. LCA results indicated that neutral pH and low current minimized environmental burdens, with the lowest weighted total damage (~0.3 mPt/FU), while intensive conditions significantly increased impacts. Overall, integrating EC with RSM, LCA, and cost analysis provides a comprehensive framework for designing technically effective, environmentally sustainable, and economically feasible treatment of antibiotic-contaminated waters.

Editorial responsibility: Samareh Mirkia.

Extended author information available on the last page of the article

Graphical abstract

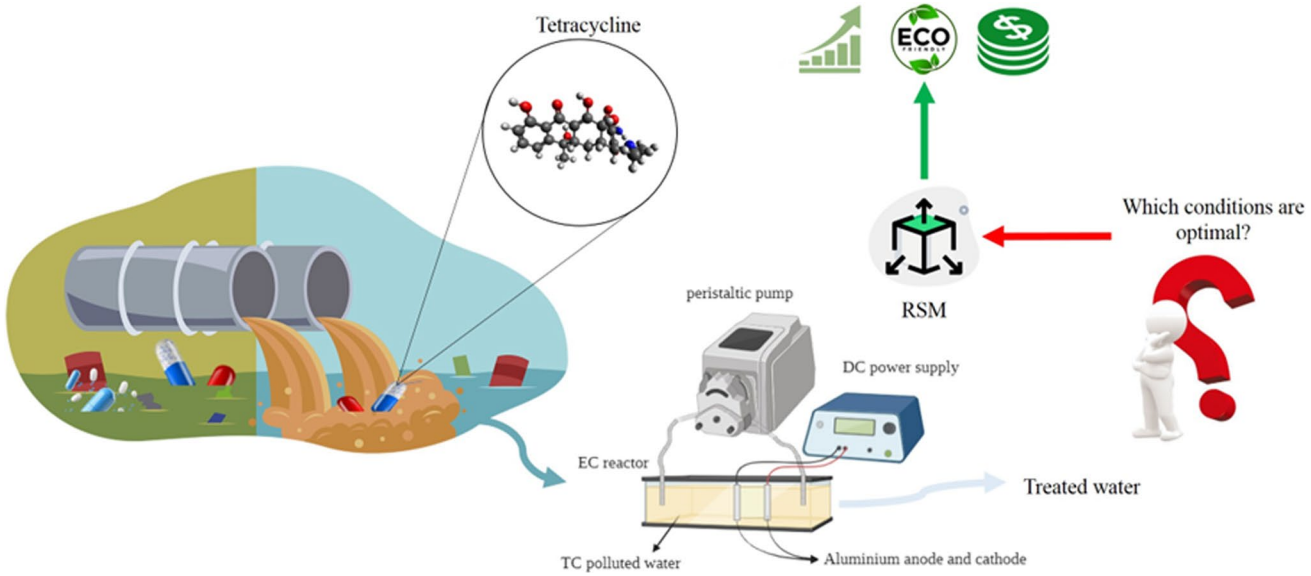

Keywords Antibiotic-contaminated water · Electrochemical treatment · Environmental impact assessment · Operational cost

Introduction

Tetracycline (TC) is one of the most widely used antibiotics for treating bacterial infections in humans and animals and is also extensively applied in livestock production and agriculture (Antos et al. 2024). According to previous reports, it ranks second globally in terms of antibiotic production and use (Lu et al. 2018). TC is currently recognised as an emerging micropollutant in various aquatic systems, including surface water, groundwater, and wastewater. Even at low concentrations, the presence of antibiotics such as TC in aquatic environments has raised considerable concern because it may contribute to the development and dissemination of antibiotic-resistant bacteria (Lu et al. 2021). The excessive and inappropriate use of antibiotics therefore poses substantial risks to environmental and public health. High levels of TC consumption have been reported in several countries and regions, including China, Germany, the European Union, and Switzerland (Al-Hashimi et al. 2022). Its persistence in the environment is exacerbated by the inefficiency of conventional wastewater treatment systems, resulting in its detection across various water matrices.

This contamination poses severe ecological risks, including harm to aquatic life and the promotion of antibiotic resistance. Given its high demand and extensive applications, TC is frequently detected in aquatic environments relative to many other pharmaceutical contaminants (Felis et al. 2020). Therefore, the development of advanced and effective remediation technologies is crucial to mitigating the environmental and health risks associated with TC pollution. Several advanced treatment methods, including membrane-based and electrochemical processes, can be energy-intensive when powered by conventional electricity. Therefore, treatment performance should be evaluated together with energy demand, operational inputs, and life cycle environmental burdens rather than considering removal efficiency alone (Al-Hashimi et al. 2023, 2022; Liu et al. 2017). In this context, electrocoagulation (EC) remains attractive because of its simple configuration, relatively low chemical requirement, and ability to generate coagulants in situ; however, its sustainability depends strongly on operating conditions such as current intensity, electrolysis time, pH adjustment, and electrode consumption (Boinpally et al. 2023; Zaied et al. 2020). Recent studies on engineered and recoverable adsorbents have also demonstrated the importance of material reusability in the sustainable removal of aqueous pollutants, indicating potential opportunities for integrating adsorption with EC in future hybrid treatment systems (Sheikh et al. 2024).

Despite these different methods, most of them rely heavily on non-renewable energy sources, which increase carbon

dioxide emissions (Boinpally et al. 2023). Among them, EC stands out as a highly effective and eco-friendly treatment method due to its chemical-free operation. It offers additional advantages, including lower setup costs, affordable electrode materials, and quicker reaction times compared to alternative techniques (Anuf et al. 2022).

Besides, this approach effectively eliminates a variety of pharmaceutical contaminants from water (Mirkhalafi et al. 2024; Zaied et al. 2020). For instance, Ensano et al. (2017) used a sacrificial aluminum anode to treat Diclofenac, carbamazepine, and amoxicillin from wastewater. Nariyan et al. (2017) employed iron and aluminum as anode and stainless steel as cathode for removing oxytetracycline hydrochloride from aqueous solutions. In an EC reactor, electrochemical oxidation and reduction reactions occur simultaneously at the anode and cathode, respectively. Aluminum is commonly used as a sacrificial electrode because its anodic dissolution produces Al^{3+} species, which subsequently undergo hydrolysis to form various monomeric and polymeric aluminum hydroxo complexes. These species destabilize dissolved and colloidal contaminants through charge neutralization, adsorption, complexation, and sweep flocculation (Anuf et al. 2022). Aluminum hydroxide precipitates are created when the produced aluminum and hydroxyl ions combine, facilitating colloidal adsorption and the floc-based removal of impurities from the aqueous phase (Tegladza et al. 2021). The EC process may be influenced by several process factors, such as pH, reaction time, current density, and electrode distance, which may affect or enhance the effectiveness of TC removal, and optimization of these parameters could increase efficiency even more.

Response surface methodology (RSM) is a set of mathematical and statistical methods used to optimize process parameters and their interactions with a few possible experiments to provide statistically significant results (Shakeri et al. 2021). RSM is primarily suited to continuous numerical variables, such as initial pH, current intensity, and reaction time, whereas categorical factors, such as electrode material, require an appropriate experimental design or separate comparative analysis. Nevertheless, RSM has been widely applied for process optimization and the prediction of operating conditions. Most studies in the literature primarily emphasize pollutant-removal efficiency. However, since EC is a current-driven process, it is crucial to optimize both removal efficiency and energy consumption in order to improve the economic feasibility of industrial-scale applications. RSM has therefore emerged as a reliable tool for process modelling, prediction, and multi-variable optimization. Its application to the removal of different contaminants has been reported by several researchers (Gadekar and Ahammed 2019; Kothari and Shah 2020) in different contaminant removal, effectively reduces the time and cost associated with experimentation. For future applications, it is essential to simulate and optimize the process to ensure its scalability and efficiency.

Although optimization at the experimental scale can improve process performance, it is not sufficient to ensure long-term sustainability. Recent pharmaceutical wastewater studies have shown that treatment technologies should be assessed not only by contaminant rejection or removal efficiency but also by their life-cycle environmental performance (Mirkhalafi et al. 2025). To address this gap, several analytical frameworks have been developed for sustainability assessment, among which life cycle assessment (LCA) is considered the most comprehensive. LCA provides a systematic methodology to quantify the environmental impacts associated with both inputs (e.g., energy and raw materials) and outputs (e.g., emissions to air and water) (Wang et al. 2024). Depending on the defined system boundaries, LCA can evaluate impacts across different life cycle stages rather than focusing solely on direct energy consumption (Hassaan et al. 2023), helping to identify opportunities for system improvement (Barbhuiya and Das 2023) and providing a basis for comparing alternative technologies. It also serves as a decision-support tool by highlighting key challenges and trade-offs that guide future research and policy (Ribeiro et al. 2024). When combined with process-level optimization techniques such as RSM, LCA links laboratory-scale efficiency with system-wide sustainability. RSM fine-tunes operational conditions, while LCA extends the evaluation to energy use, electrode wear, and waste generation over the life cycle. Together, they offer a framework for designing EC systems that are technically effective, cost-conscious, and environmentally sustainable.

Although different EC materials have been applied in previous studies to remove TC from water, most investigations have focused primarily on treatment performance, with limited consideration of how optimized operating conditions affect life-cycle environmental burdens and operational cost. Recent studies have begun to couple EC process optimization with LCA for selected wastewater treatment applications. For example, Sedaghat et al. (2025) optimized an EC process for industrial/textile wastewater treatment and evaluated its environmental impacts using LCA, demonstrating the value of linking process optimization with sustainability assessment. In addition, LCA has been applied to EC-based treatment systems such as electrocoagulation–ozonation for textile wastewater and EC for greywater treatment, further showing the relevance of life-cycle thinking for electrochemical water treatment systems (Ahangarnokolaei et al. 2021; Patel et al. 2023). However, the direct integration of BBD-RSM optimization, LCA, and operational cost analysis remains rarely addressed for antibiotic-contaminated waters, particularly for TC removal. To address this gap, the present study combines EC, RSM, LCA, and operational cost analysis into a single framework for TC removal from water. EC

was conducted using aluminum electrodes as both anode and cathode, while RSM, based on the Box–Behnken design (BBD), was employed to optimize the key operating parameters and identify the operating region that balances TC removal efficiency with energy and material requirements. In parallel, LCA was applied to evaluate the environmental performance of the process from a cradle-to-gate perspective, and an economic assessment was performed to estimate operational costs, including energy, electrode, and chemical consumption. By combining these approaches, this study establishes an integrated decision-support framework that not only targets maximum TC removal but also identifies the trade-offs between treatment efficiency, environmental burden, and operational cost, highlighting practical limitations and the broader applicability of EC for antibiotic-contaminated waters.

Materials and methods

Tools and chemicals

Materials that have been used for this study are listed in this section. The set of EC experiment equipment includes a 1.2 L bench-scale reactor, a peristaltic pump made by Watson Marlow (504 U), and a DC power supply made by British Standard Tester (BTS 2/5A, two two-channel regulated). Each aluminum electrode measured 55 mm in width, 110 mm in height, and 1 mm in thickness, with 35 perforations of 0.5 cm diameter arranged in ten rows. Approximately 80% of each electrode was submerged, giving an effective submerged electrode area of 180 cm^2 for the pair, with an inter-electrode spacing of 0.5 cm and an immersion depth of 8.8 cm. Before each experiment, the electrodes were cleaned with HCl and lightly abraded with sand filters to prevent cross-contamination and restore surface activity. All the samples were measured with a spectrophotometer (DR 3900 UV–Vis, Hach, Germany) after filtering with Whatman filter paper grade (1) at a diameter of 90 mm. Also, HCL (32%), NaOH, and TC, with the chemical formula $C_{22}H_{24}N_2O_8$.HCL powder was purchased from Sigma-Aldrich, Merck, Germany.

Experimental set-up of batch sequential EC and procedure

The experiment was conducted by pouring a one-liter beaker with DI water, stirring it, and then adding 50 mg of TC per Liter based on the previous literature on TC (Al-Hashimi et al. 2023, 2022). Various conditions, such as pH (3–11), electrolysis time (5–30 min), inter-electrode distance (5–15 mm), and current intensity (10–30 mA), have been tested during the experiment and based on the output of the RSM model. The selected operating ranges

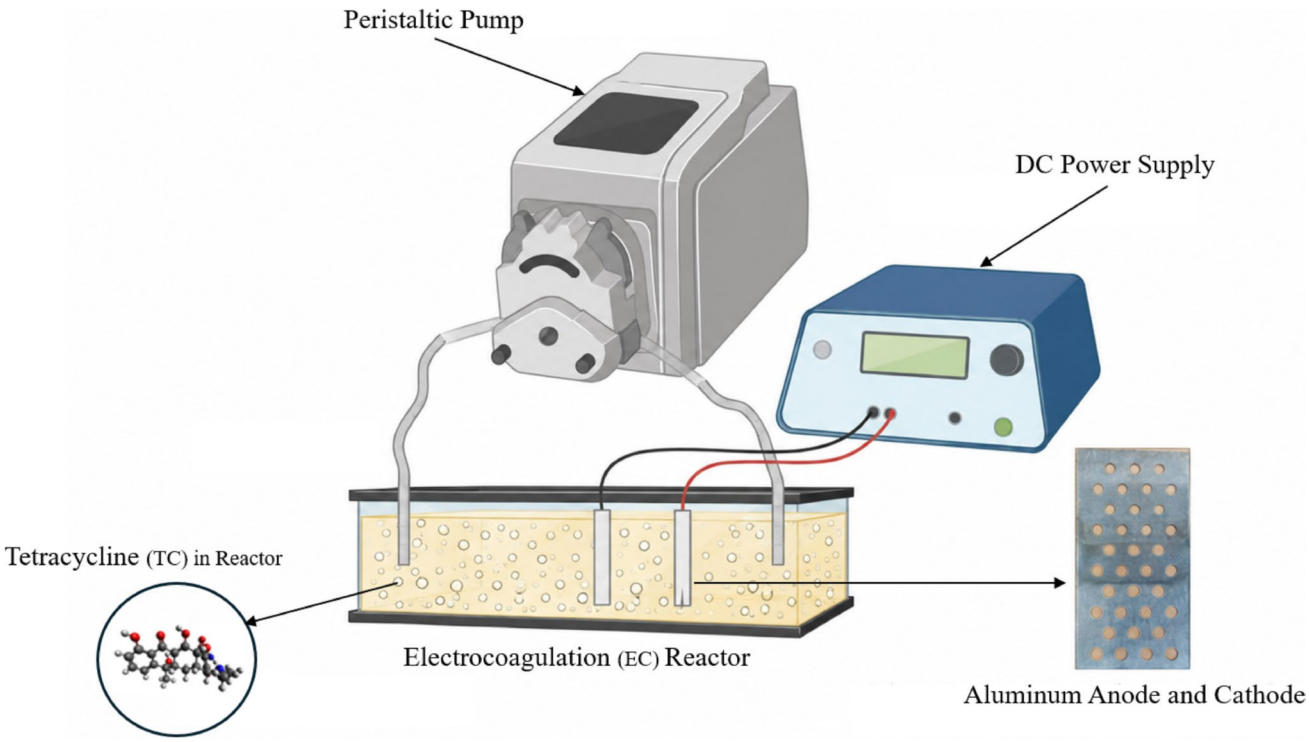

Fig. 1 Experimental Setup utilized for this work

were chosen based on previous EC studies on pharmaceutical removal, including our earlier EC-based treatment work, and preliminary feasibility considerations (Mirkhalafi et al. 2024). By adding HCL and NaOH, respectively, the pH of the solution was brought below and above neutral, between 3 and 11. The setup for the experiment is shown in Fig. 1. A pump was used to circulate water between the two aluminum electrodes, each with a surface area of approximately 60cm^2. The electrodes were connected to a direct current power supply, which provided an adjustable voltage range of 0–30 V and a current range of 0–3 A.

At specified time intervals during each run, a 10 mL sample was extracted from the center of the reactor using a syringe. The sample was then filtered through filter paper and analyzed using a UV spectrophotometer. The removal efficiency of GW was determined using the following Eq. (1) (Olya and Pirkarami 2013):

$$R_e(\%) = \frac{(C_0 - C_t)}{C_0} \times 100 \quad (1)$$

where C_0 and C_t are the initial and final concentrations of TC, respectively.

Response surface methodology (RSM)

Factorial designs are limited to predicting the linear trends of variables and cannot account for curvature or identify critical points within the experimental space. To address this limitation, RSM was employed to model the process. RSM allows for a precise analysis of variables in various formats while minimizing the number of experimental runs required. The BBD was selected over other RSM designs because it avoids experiments at extreme factor combinations, which are often impractical or unstable in electrocoagulation systems. Designs such as the central composite design include axial points that may require very high current densities, extreme pH values, or prolonged electrolysis times, leading to electrode passivation, excessive energy consumption, and unreliable operation. BBD restricts all experiments to a safe and feasible operating range while still enabling accurate estimation of quadratic effects and interactions with a reduced number of runs. Given the experimental cost, electrode consumption, and the objective of optimizing performance within a realistic operating window, BBD was considered the most appropriate design for this study.

Table 1 Experimental range and levels of independent process parameters for Box-Behnken design

Variables	Unit	Symbols (uncoded)	Coded levels		
			−1	0	+1
pH	-	A	3	7	11
Electrolysis time	min	B	5	17.5	30
Inter-electrode distance	mm	C	5	10	15
Current intensity	mA	D	10	20	30

RSM and BBD are powerful statistical techniques commonly used for modeling and optimizing the combined effects of key parameters within a four-factor, three-level framework. These three levels include one axial point, one factorial point, and one central point for each variable. The number of experiments is determined based on the number of variables, as outlined in the following Eq. (2) (Kothari et al. 2022):

$$E = 2^v + 2V + P \quad (2)$$

where E is the number of demanded experiments for analysis, V is the number of independent variables, and P is the number of replications at the central point. A total of 29 trials were planned based on a framework comprising four variables and three levels. The relationship between the response variable (y) and the independent variables was modeled using a second-order polynomial regression equation, as represented in Eq. (3), to examine their interactions comprehensively (Silva et al. 2011).

$$y = \beta_0 + \sum_{i=1}^{k} \beta_i x_i + \sum_{i=1}^{k} \beta_{ii} x_i^2 + \sum_{1 \le i \le j}^{k} \beta_{ij} x_i x_j + \varepsilon \quad (3)$$

where y determines the result (removal efficiency of TC in percentage), j is second-order, I is the linear constant, β_0 is a constant coefficient, β_i is the regression constant, β_{ii} is the quadratic coefficient, and β_{ij} is the interaction coefficient. Also, x_i and x_j are the coded independent variables.

In this study, BBD with five-level factors was utilized, comprising 27 experimental trials generated using Minitab software (version 22.1.0). The design featured four axial points, 20 factorial points, and three central point replications, focusing on optimizing %TC using the EC-aluminum method. Key input factors, namely pH (3–11), electrolysis time (5–30 min), inter-electrode distance (5–15 mm), and current intensity (10–30 mA) were considered, and these factors were assigned labels of − 1 (low), 0 (center), 1 (high) (refer to Table 1). The independent variables were standardized using Eq. (4) (Igwegbe et al. 2024):

$$X_i = \frac{(X_i - X_0)}{\Delta X} \times 100 \quad (4)$$

where X_i denotes the coded dimensionless value of the variable, X_0 represents the variable's value at the central point, and ΔX indicates the step increment.

Although acidic pH values were expected to reduce TC removal, pH 3 was intentionally included to define the lower

boundary of the design space and to capture the transition in TC speciation and aluminum hydrolysis behavior. Including low-performance regions is necessary in RSM to estimate curvature and identify the true optimum within the selected range.

Life cycle assessment (LCA)

According to ISO (2006a, 2006b), LCA has four phases: (i) goal and scope definition, (ii) life cycle inventory (LCI), (iii) life cycle impact assessment (LCIA), and (iv) interpretation. This framework ensures transparency, reproducibility, and comparability across studies (He et al. 2023). The objective of this study is to couple RSM-derived optimal conditions with an LCA framework, enabling a dual evaluation, including achieving the highest possible TC removal efficiency while minimizing overall environmental impacts. In this study, the functional unit (FU), used as the basis for normalizing all inputs and outputs, is defined as the treatment of 1 m^3 of water containing 50 g of TC.

A cradle-to-gate perspective was adopted, covering activities from wastewater preparation (TC in deionized water, pH adjustment with HCl/NaOH) to EC operation. The boundary starts with TC-contaminated water entering the reactor and ends with its removal. Upstream processes (electricity, electrodes, chemicals) were included; downstream (waste disposal) was excluded due to the lab scale. Notably, LCA has two main approaches, including attributional (ALCA) and consequential (CLCA). ALCA evaluates the environmental impacts of material and resource flows using average data within fixed system boundaries, making it suitable for scenario comparison (Finnveden et al. 2009; Kiehbadroudinezhad et al. 2023). This study adopts an ALCA approach.

The LCI, as the second phase of an LCA, forms the foundation of any LCA analysis (Wang et al. 2024). Inventory analysis involves collecting, processing, and organizing data to quantify inputs and outputs, identify environmental hotspots, and generate evidence-based recommendations (Shang et al. 2024).

Background data refer to flows associated with the production of materials and energy carriers and are typically sourced from validated databases (herein, EcoInvent v3). Foreground data were also directly collected from laboratory experiments, with operational conditions derived from RSM optimization to ensure consistency between experimental efficiency and environmental assessment.

LCIA, the third phase of LCA, translates substance flows from LCI into specific impact categories to assess potential environmental impacts (Rosenbaum et al. 2018). This study used ReCiPe2016 within SimaPro (v.9) to model inventory data and convert substance flows into impact categories. Although ReCiPe 2016 provides both midpoint and endpoint results, this study focused exclusively on endpoint indicators. Midpoint indicators, while detailed, can be challenging to interpret due to their abstract nature and the large number of categories, especially when comparing multiple scenarios (Loya-González et al. 2019). Endpoint results were normalized and weighted into a single score (mPt) for direct scenario comparison, reflecting the overall environmental burden and linking RSM optimization with environmental sustainability.

Operational cost estimation

Operational cost (OPC) is a crucial parameter for assessing the economic feasibility of the EC process at pilot and industrial scales. In this study, the operational cost was estimated by accounting for three major contributors: energy consumption, electrode dissolution, and chemical consumption (NaCl electrolyte). All costs were expressed in £ per m^3 of treated water based on UK market prices. The total OPC was calculated using Eq. (5):

$$OPC\left(£/m^3\right) = [a \times EEC] + [b \times EC] + [c \times CC] \quad (5)$$

where a is the UK average business electricity tariff of £0.253 per kWh (£/kWh), b is the London Metal Exchange (LME) benchmark price of £2.10 per kg of aluminum (£/kg), and c is the chemical cost of NaCl, which was taken as £20 per kg (lab-grade) (£/kg). EEC is the electrical energy consumption (kWh/m^3), EC is the electrode consumption (kg/m^3), and CC is the chemical consumption (kg/m^3). The electrical energy consumption was calculated from the applied current, voltage, time, and reactor volume (Eq. 6):

$$EEC\left(kWh/m^3\right) = (U \times I \times t)/(\left(C_0 - C_t\right) \times \left(V_R\right) \quad (6)$$

where EEC is electrical energy consumption, U is the applied voltage (V), I is the current (A), t is the electrolysis time (h), and VR is the reactor volume (L).

The electrode consumption (EC) was estimated using Faraday's law of electrolysis (Eq. 7):

$$EC\left(kWh/m^3\right) = \left(M_v \times I \times t\right)/(Z \times F \times \left(C_0 - C_t\right) \times \left(V_R\right) \quad (7)$$

where EC is electrode consumption, M is the molar mass of aluminum (26.98 g/mol), z is the number of electrons transferred (z = 3 for Al^{3+}), and F is Faraday's constant (96,485 C/mol). Finally, the chemical consumption was calculated from the mass of NaCl added per unit volume of treated water (Eq. 8):

$$CC\left(kg/m^3\right) = mNACL/\left(V_R\right) \quad (8)$$

where CC is chemical consumption, mNaCl is the mass of NaCl used (kg). This framework allows accurate determination of operating costs by integrating all major contributors under UK conditions.

Table 2 BBD experimental design and the response results for TC removal using the EC process

Run	pH	Current (mA)	Distance (mm)	Time (min)	Predicted Removal (%)	Actual Removal (%)
1	7	20	5	30	89.5	90.9
2	11	20	10	30	99.8	100.0
3	7	10	15	17.5	74.6	74.4
4	7	20	5	5	74.8	74.1
5	3	10	10	17.5	54.2	47.4
6	7	20	15	30	95.0	93.1
7	3	20	15	17.5	60.8	57.0
8	7	20	10	17.5	91.1	86.8
9	11	10	10	17.5	108.7	98.6
10	3	20	5	17.5	57.5	50.1
11	11	30	10	17.5	94.9	99.2
12	11	20	15	17.5	93.3	100.0
13	7	30	5	17.5	79.4	82.9
14	7	30	10	30	107.9	95.6
15	7	30	10	5	77.6	72.2
16	7	30	15	17.5	91.1	93.9
17	7	10	10	30	91.6	96.4
18	11	20	5	17.5	95.3	98.3
19	7	10	5	17.5	85.0	85.4
20	7	20	15	5	70.6	66.7
21	7	20	10	17.5	91.1	95.6
22	11	20	10	5	103.7	99.4
23	7	10	10	5	82.9	94.5
24	3	20	10	30	88.1	95.6
25	3	20	10	5	45.1	48.2
26	7	20	10	17.5	91.1	90.9
27	3	30	10	17.5	79.0	86.5

Results and discussion

RSM experimental design

A BBD was employed to evaluate the combined effects of four independent variables, initial pH, current density, inter-electrode distance, and electrolysis time, on TC removal efficiency by the EC process. The experimental matrix consisted of 27 runs, as presented in Table 2. Each factor was studied at three levels, and five of the runs (Run 3, Run 7, Run 15, Run 19, and Run 23) were conducted at the central point (pH 7, current 20 mA, distance 10 mm, and time 17.5 min) to provide an estimate of experimental error and assess the adequacy of the model.

The predicted removal efficiencies obtained from the quadratic regression model were in close agreement with the actual experimental data, indicating the reliability of the RSM approach in modelling the EC process. Actual removal values ranged from 47.4% to 100%, while predicted removals were within a similar range (45.1%–108.7%). This close correlation highlights the suitability of the BBD for optimizing process parameters and supports the robustness of the developed model in describing the relationship between operating conditions and TC removal efficiency.

Development and validation of RSM models

The derived model and its parameters were evaluated using the analysis of variance (ANOVA) technique. Table 3 presents the results obtained from the ANOVA calculations. These calculations are based on the experimental data generated from each run, which were then used to determine the significance of the individual terms included in the quadratic model. For each source of variation, the mean square was calculated by dividing its sum of squares by the corresponding degrees of freedom (df). The degrees of freedom represent the number of independent pieces of information

Table 3 ANOVA results of the quadratic for TC removals

Source	DF	Seq SS	Contribution	Adj SS	Adj MS	F-Value	*P*-Value
Model	14	6639.17	88.67%	6639.17	474.23	6.70	0.001
Linear	4	4927.70	65.81%	4927.70	1231.93	17.42	0.000
pH	1	3701.08	49.43%	3701.08	3701.08	52.33	0.000
Cur	1	94.13	1.26%	94.13	94.13	1.33	0.271
Dis	1	0.91	0.01%	0.91	0.91	0.01	0.912
Time	1	1131.58	15.11%	1131.58	1131.58	16.00	0.002
Square	4	524.36	7.00%	524.36	131.09	1.85	0.184
pH*pH	1	136.35	1.82%	214.89	214.89	3.04	0.107
Cur*Cur	1	16.82	0.22%	1.49	1.49	0.02	0.887
Dis*Dis	1	369.49	4.93%	344.32	344.32	4.87	0.048
Time*Time	1	1.69	0.02%	1.69	1.69	0.02	0.880
2-Way Interaction	6	1187.12	15.85%	1187.12	197.85	2.80	0.061
pH*Cur	1	371.86	4.97%	371.86	371.86	5.26	0.041
pH*Dis	1	6.85	0.09%	6.85	6.85	0.10	0.761
pH*Time	1	548.31	7.32%	548.31	548.31	7.75	0.017
Cur*Dis	1	121.42	1.62%	121.42	121.42	1.72	0.215
Cur*Time	1	115.43	1.54%	115.43	115.43	1.63	0.226
Dis*Time	1	23.24	0.31%	23.24	23.24	0.33	0.577
Error	12	848.75	11.33%	848.75	70.73		
Lack-of-Fit	10	809.85	10.82%	809.85	80.98	4.16	0.209
Pure Error	2	38.91	0.52%	38.91	19.45		
Total	26	7487.92	100.00%				

associated with each source of variation. The mathematical model predicts the response (TC removal efficiency) under a defined set of experimental conditions. As expected, these predictions differ slightly from the actual experimental results. The differences between the predicted and observed values are referred to as residuals. The statistical significance of each model term was assessed using the F-value, calculated as the ratio of the mean square of the term to the mean square of the residual error. A large F-value indicates that the variation explained by the term is substantial relative to the unexplained experimental error. Generally, a model term is considered statistically significant when its associated p-value is below 0.05 at the 95% confidence level.

In this study, the overall model was found to be statistically significant, with an F-value of 6.70 and a corresponding p-value of 0.001 (<0.0001). In RSM, an insignificant lack-of-fit value generally indicates that the selected regression model adequately represents the experimental design space (Jensen 2017). In the present study, the lack of fit was not significant ($p=0.209>0.05$), confirming that the quadratic model was suitable for describing TC removal under the investigated conditions. Therefore, the model can be considered acceptable and reliable for predicting TC removal by EC.

Residual analysis was used to evaluate whether the model assumptions were satisfied. The residuals were randomly distributed around zero, indicating that the differences between predicted and experimental values were mainly associated with random experimental error rather than systematic bias. Similar residual diagnostic approaches, normal probability plots and predicted-versus-actual comparisons were reported by Kumari and Gupta (Kumari and Gupta 2019) during RSM optimization of trihalomethane and natural organic matter removal from drinking water using surfactant-modified magnetic nano adsorbents, where these analyses were applied to evaluate model adequacy and prediction reliability. The p-values of the individual model terms were also examined, and it was found that the most influential factors had $p<0.0001$, indicating strong significance (Ansari et al. 2022). Overall, the statistical evaluation demonstrates that the developed quadratic model is highly significant, well-fitted, and capable of accurately describing the relationship between operating parameters and TC removal efficiency.

$$\begin{aligned}\text{Re:} &- 37.4 + 19.52\,pH + 0.32\,Cur + 4.06\,Dis \\ &+ 1.30\,Time - 0.397\,pH * pH - 0.0053\,Cur * Cur \\ &- 0.321\,Dis * Dis - 0.0036\,Time * Time \\ &- 0.241\,pH * Cur - 0.065\,pH * Dis \\ &- 0.2342\,pH * Time + 0.1102\,Cur * Dis \\ &+ 0.0430\,Cur * Time + 0.0386\,Dis * Time\end{aligned}$$

The quadratic model explained 88.67% of the total variation in TC removal, corresponding to $R^2=0.887$. Based

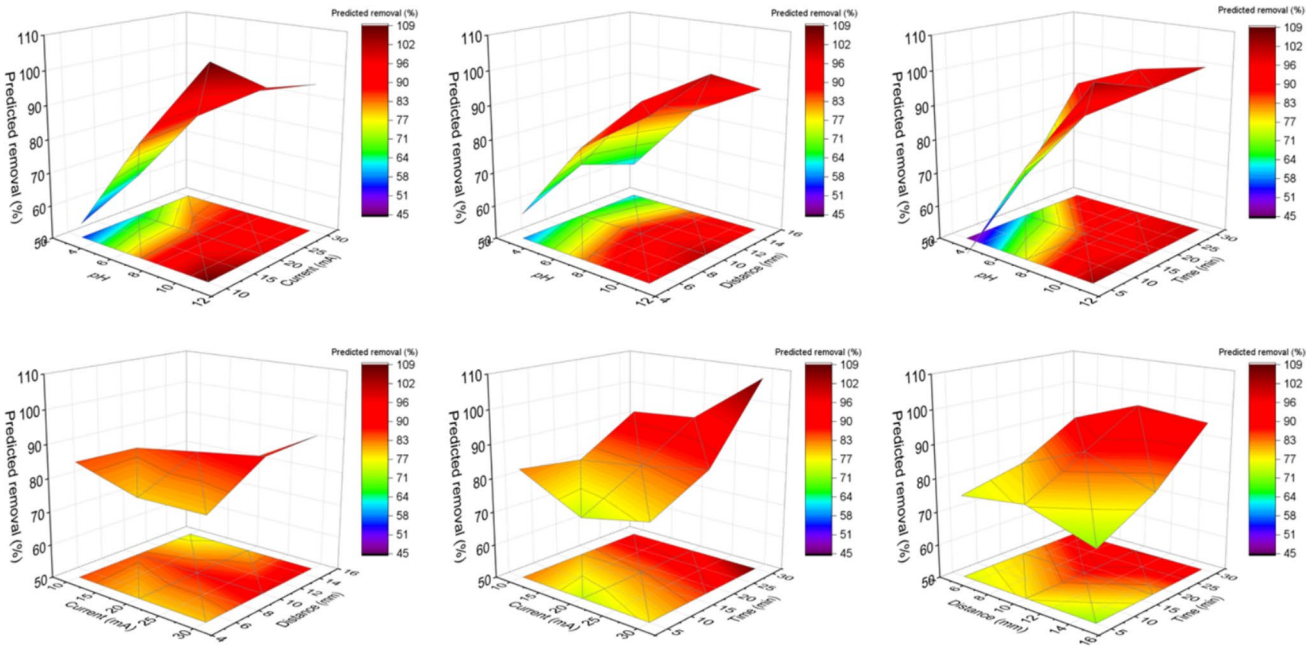

Fig. 2 Response surface plots showing the interactive effects of operational parameters on TC removal efficiency by electrocoagulation. **a** Effect of pH and current density; **b** Effect of pH and inter-electrode distance; **c** Effect of pH and electrolysis time; **d** Effect of current density and inter-electrode distance; **e** Effect of current density and electrolysis time; (**f**) Effect of inter-electrode distance and electrolysis time

on the ANOVA results, the overall model was significant ($F = 6.70$, $p = 0.001$), while the lack of fit was not significant ($p = 0.209$), confirming model adequacy. Among the linear terms, pH and electrolysis time were significant, whereas current intensity and inter-electrode distance were not significant as individual linear factors. Among the quadratic terms, only Dis^2 was significant. For interaction terms, pH × current and pH × time were significant, while pH × distance, current × distance, current × time, and distance × time were not significant. Although some terms were statistically nonsignificant, they were retained in the full quadratic model to preserve model hierarchy and allow interpretation of interaction and curvature effects.

Data analysis via RSM

Figure 2 presents the 3D surface plots showing the interaction effects of operating variables on TC removal efficiency by EC. The subplots (a–f) illustrate the combined influence of pH, current density, inter-electrode distance, and electrolysis time on predicted removal.

Effect of pH and current density

As can be seen from Fig. 2a, the removal efficiency of TC is low at acidic pH (below 6) and low current densities (< 10 mA). As both pH and current density increase, removal efficiency rises sharply, reaching > 95% at pH 7–9 and current density above ~ 20 mA. Beyond this region, removal remains nearly constant, suggesting a plateau. At acidic pH, limited hydrolysis of aluminum restricts floc formation, while increasing pH promotes the formation of amorphous $Al(OH)_3$ flocs with high surface area, which enhance adsorption and charge neutralization. This observation is consistent with aluminum speciation and TC equilibrium behavior reported in the literature: at very low pH (2–3), cationic Al species (Al^{3+}, $Al(OH)^{2+}$) dominate, while TC exists mainly as a cationic form, leading to electrostatic repulsion and poor removal. The low removal observed at pH < 4 confirms the importance of including acidic conditions in the design space, as these runs helped define the lower-performance boundary and contributed to the estimation of model curvature. Between pH 4–10, a range of monomeric and polymeric aluminum hydroxy species (e.g., $Al(OH)_2^+$, $Al_6OH_{15}^{3+}$, $Al_{13}OH_{34}^{5+}$) form and progressively convert into amorphous $Al(OH)_3(s)$, enabling efficient charge neutralization and adsorption of TC. At alkaline conditions (pH > 7.7), TC exists predominantly as anionic species, which are strongly attracted to the cationic hydrolysis products and adsorbed onto $Al(OH)_3$ flocs, leading to maximum removal efficiency (Ait Ouaissa et al. 2014; Zhang et al. 2011). On the other hand, higher current density increases the rate of coagulant and microbubble generation, as well as promoting electron transfer and hydroxyl radical (OH) formation, thereby improving TC destabilization. However, beyond ~ 20 mA, the increase becomes marginal because side reactions (such as OH self-quenching to O_2 and shifts in cathodic reduction pathways) reduce oxidant utilization,

while electrode passivation and bubble shielding further limit efficiency, leading to a plateau and higher energy consumption (Dong et al. 2021).

Effect of pH and inter-electrode distance

Figure 2b shows the interaction effect of pH and inter-electrode distance. Removal efficiency remains poor under acidic conditions, regardless of electrode distance. At neutral–alkaline pH, efficiency improves significantly and is highest (> 95%) at shorter electrode distances (~ 5–10 mm). A relatively short electrode gap can reduce the electrical resistance of the solution and the voltage required to maintain a given current. However, excessively narrow spacing may restrict liquid circulation, promote the local accumulation of gas bubbles and flocs, and reduce effective mass transfer within the inter-electrode region. Mousazadeh et al. (2021) reviewed EC studies and reported that inter-electrode distance strongly affects ohmic resistance, energy consumption, coagulant transport, and pollutant removal efficiency. Their review showed that shorter electrode gaps commonly improve EC performance by reducing solution resistance, although excessively narrow gaps may restrict flow and bubble release. Increasing the spacing beyond this optimum leads to reduced removal efficiency, as mass transfer is limited and resistance increases, resulting in less effective floc formation and higher energy consumption. Atashzaban et al. (2016) reported that increasing electrode spacing from 1 to 3 cm decreased COD and TSS removal with both iron and aluminum electrodes, with the best removal at 1 cm. Similarly, removal efficiencies over 87% for COD, TSS, color, and phosphate were observed at a 0.5 cm spacing (Naje et al. 2015). Thus, while Fig. 2b demonstrates that TC removal is maximized at shorter electrode distances under neutral–alkaline pH, in agreement with previous studies showing that the electrode gap should be optimized to balance pollutant removal, hydraulic conditions, and electrical energy demand.

Effect of pH and electrolysis time

Figure 2c illustrates the interaction between pH and electrolysis time on TC removal. At acidic pH values, removal efficiency remains relatively low even with extended treatment, which can be attributed to the limited hydrolysis of aluminum and the predominance of cationic TC species that hinder adsorption. In contrast, under neutral to alkaline conditions, efficiency increases steadily with time, reaching values above 95% at ~ 15–20 min. Beyond this point, the curve flattens, suggesting limited further improvement. Neutral-to-alkaline pH favors the generation of insoluble $Al(OH)_3$ species that act as efficient adsorbents, and extended electrolysis time promotes greater coagulant formation and stable floc development.

This observation is consistent with prior studies showing that extending the electrolysis duration enhances the removal of COD, TOC, turbidity, and other pollutants by producing more hydroxide flocs and enabling charge neutralization. For example, Hawari et al. (2020) reported that TOC removal efficiency increased steadily with electrolysis time, rising from less than 25% at 5 min to over 80% at 60 min, as greater quantities of metal hydroxides were produced and facilitated pollutant coagulation and adsorption. However, once near-maximum pollutant destabilization is reached, additional electrolysis offers little benefit and may even reduce efficiency. This has been attributed to (i) depletion of available contaminants, (ii) reduction in the concentration of polymeric Al hydroxy complexes responsible for charge neutralization, and (iii) the formation of more soluble ionic species that decrease floc stability (Janpoor et al. 2011). Moreover, prolonged operation substantially increases energy consumption without proportional improvement in removal performance. Therefore, although increasing electrolysis time enhances TC removal under neutral–alkaline conditions, the process exhibits diminishing returns beyond approximately 20 min. Selecting an optimum electrolysis time is thus essential for balancing treatment efficiency and energy consumption.

Effect of current density and inter-electrode distance

Figure 2d illustrates the interaction between current density and inter-electrode distance on TC removal by EC. At lower current densities (< 15–20 mA), the removal efficiency remains moderate, around 75–85%, regardless of electrode spacing. This behavior is consistent with Ait Ouaissa et al. (2014), who found that under low current densities, TC removal was limited even when electrode spacing was small (their work showed modest improvement only when current density was increased). As the current density increases beyond 20 mA, removal efficiency improves significantly, particularly when the electrode spacing is short (4–10 mm), where efficiencies approach 90%. Under these conditions, the rate of aluminum dissolution and coagulant production is enhanced, and the shorter distance between electrodes minimizes ohmic resistance and promotes effective interaction between coagulants and TC molecules. In contrast, at wider electrode distances (> 12 mm), removal efficiency remains relatively unchanged even as current density increases, generally stabilizing around 80–85%. This may be attributed to the higher electrical resistance associated with larger electrode spacing, which increases the required cell voltage and may reduce the effective transport and distribution of coagulant species within the reactor. As a result, increasing the applied current density under these conditions produces only limited additional improvement in TC removal. Similar behavior was observed by Almukdad et al. (2021), who reported that Fe and Mn removal percentages decreased notably when the electrode spacing was increased from 0.5 to 1.5 cm under fixed current and time, attributing the decline to increased electrical resistance and reduced dissolution of the coagulant from the electrodes. Overall, the optimum conditions for TC removal were observed at higher

current densities (25–30 mA) combined with shorter electrode spacing (5–10 mm), where the synergistic effect of enhanced coagulant generation and efficient transport processes resulted in maximum removal performance.

Effect of current density and electrolysis time

Figure 2e illustrates the interaction between current density and electrolysis time on TC removal by EC. At low current density (< 15 mA), removal efficiency remains modest even when the reaction time is extended, indicating that insufficient coagulant production limits pollutant destabilization. In contrast, when the current density is increased above 20 mA, the effect of electrolysis time becomes more pronounced: removal efficiency rises steadily with treatment duration, exceeding 95% after ~ 20–25 min. This demonstrates the synergistic effect of the two parameters: higher current density accelerates aluminum dissolution and hydroxyl radical generation, while longer electrolysis time allows these species to accumulate and interact effectively with TC molecules. However, extending both parameters beyond ~ 25–30 mA and ~ 25–30 min does not substantially improve removal, reflecting diminishing returns. At high current densities, the rapid generation of coagulant species may exceed the amount required for pollutant removal, while intensified gas evolution and bubble accumulation may interfere with floc formation and separation. Similar behavior has been reported in Bazrafshan et al. (2013), who found that COD and turbidity removal in dairy wastewater increased significantly with both higher current and longer treatment, up to an optimum time beyond which the efficiency stabilized. Furthermore, extending electrolysis time under high current densities substantially increases energy consumption, raising operational costs without significant performance improvement (Al-Qodah et al. 2025). In summary, maximum TC removal efficiency (> 95%) is achieved at a current density of ~ 25–30 mA combined with an electrolysis time of ~ 20–25 min, indicating that these conditions provide a favourable balance among coagulant generation, contact time, removal efficiency, and energy demand.

Effect of inter-electrode distance and electrolysis time

Figure 2f shows the combined effect of electrolysis time and inter-electrode distance on TC removal by EC. At shorter reaction times (< 10 min), removal efficiency is moderately low (60–75%), especially when electrode spacing is large (> 12 mm), since insufficient time does not allow adequate accumulation of aluminum hydroxide flocs, and increased ohmic resistance at wider spacing further impairs effective coagulant production and transport. As electrolysis time increases (> 20 min), removal efficiency improves across all spacings but is especially enhanced at shorter distances (~ 5–10 mm), where removal exceeds 90% due to more effective floc generation and pollutant-coagulant interaction. Wider electrode gaps (> 12 mm) show less improvement even with prolonged time, with efficiencies stabilizing around 80–85%. This behavior is consistent with Al-Kilani and Bani-Melhem (2025), who reported that increasing electrode distance increased energy consumption but did not enhance removal efficiency significantly. Similarly, Zhang et al. (2022) in their study on TC removal from livestock wastewater found that using an electrode spacing of 1 cm under pulse-current EC achieved ~ 95% removal when appropriate current intensity and treatment duration were deployed, which aligns with the trend seen in our data. Overall, the optimum removal for TC in this study is achieved when electrolysis time is extended to ~ 20–25 min and electrode spacing is close (~ 5–10 mm), where transport

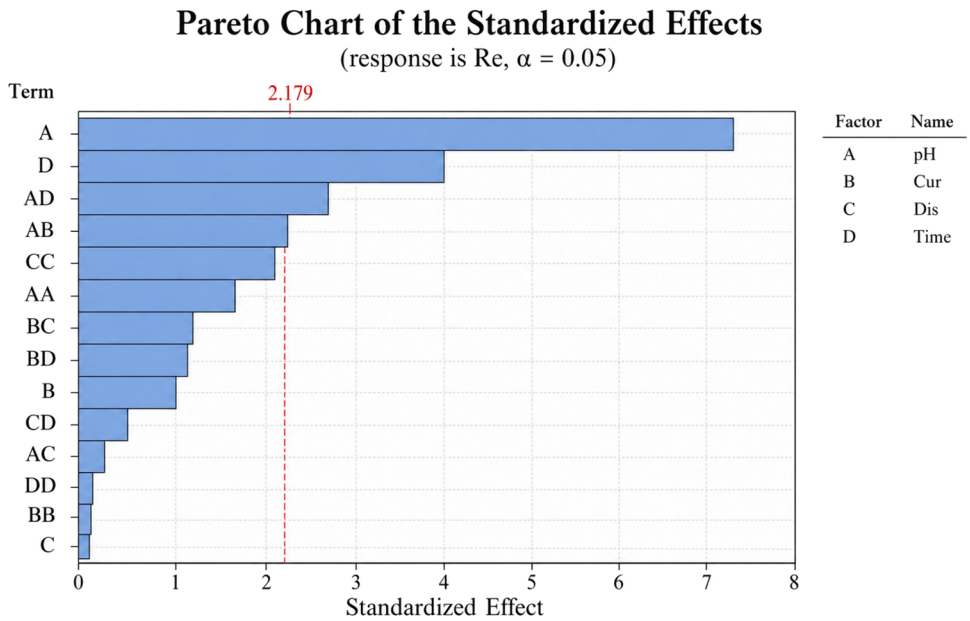

Fig. 3 Pareto chart of the standardized effects showing the relative significance of pH (**A**), current (**B**), distance (**C**), and time (**D**) on TC removal efficiency (Re) at α = 0.05

processes and floc formation are maximized while resistance is minimized.

Pareto chart analysis

The Pareto chart (Fig. 3) quantitatively ranked the influence of key operating parameters on TC removal efficiency during EC. Among the tested variables, pH exhibited the highest standardized effect, identifying it as the most critical factor controlling TC removal. Electrolysis time ranked second, followed by the combined interaction of pH and time, indicating that both the solution chemistry and reaction duration synergistically govern process performance. The interaction between pH and electrolysis time (pH × Time) slightly exceeded the significance threshold, indicating a moderate interaction effect on TC removal performance. In contrast, the interaction between pH and current intensity (pH × Cur) was located close to the significance boundary, suggesting a comparatively weaker contribution. Inter-electrode distance (Dis) exhibited the smallest standardized effect among all investigated parameters and remained far below the significance threshold, indicating a comparatively minor influence within the studied experimental range. This outcome highlights the dominant role of pH in regulating aluminum hydrolysis, floc speciation, and TC ionization, while electrolysis time determines the extent of coagulant generation and pollutant removal. In contrast, other parameters, such as current intensity, inter-electrode distance, and their interactions, showed standardized effects below the significance threshold (2.179), suggesting their relatively minor influence under the studied conditions. Overall, the analysis confirms that optimizing pH and electrolysis time is key to achieving efficient TC removal and guiding energy-conscious design and scale-up of EC systems.

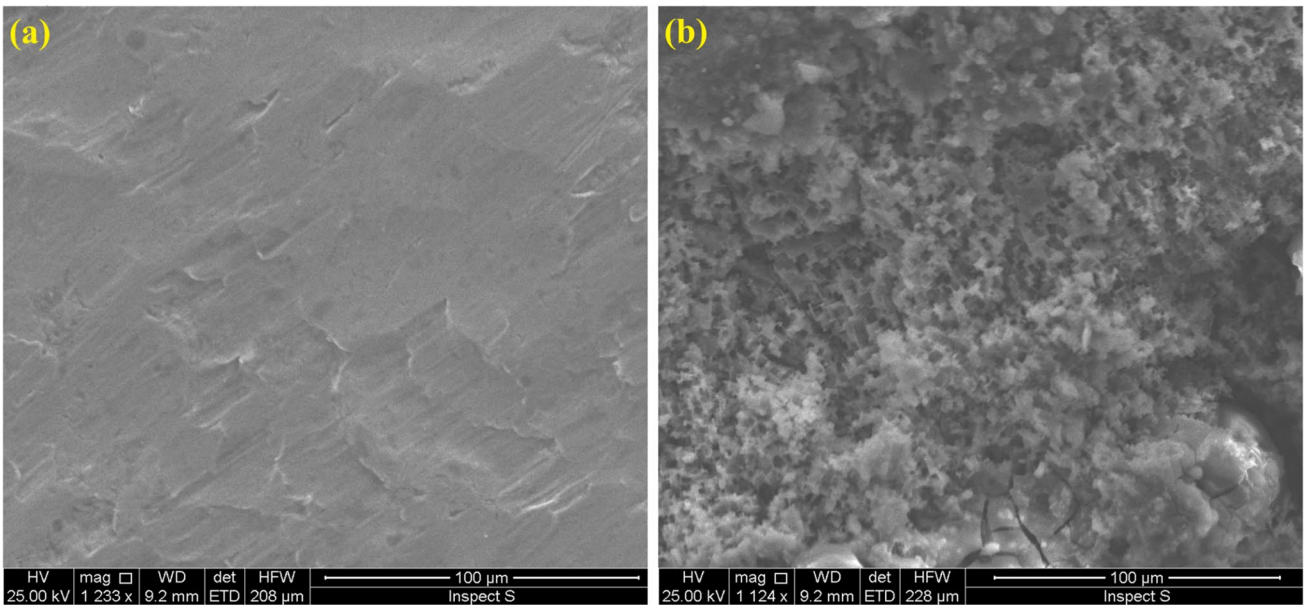

Fig. 4 Scanning electron micrographs of aluminum electrode surfaces, **a** before and **b** after electrocoagulation treatment

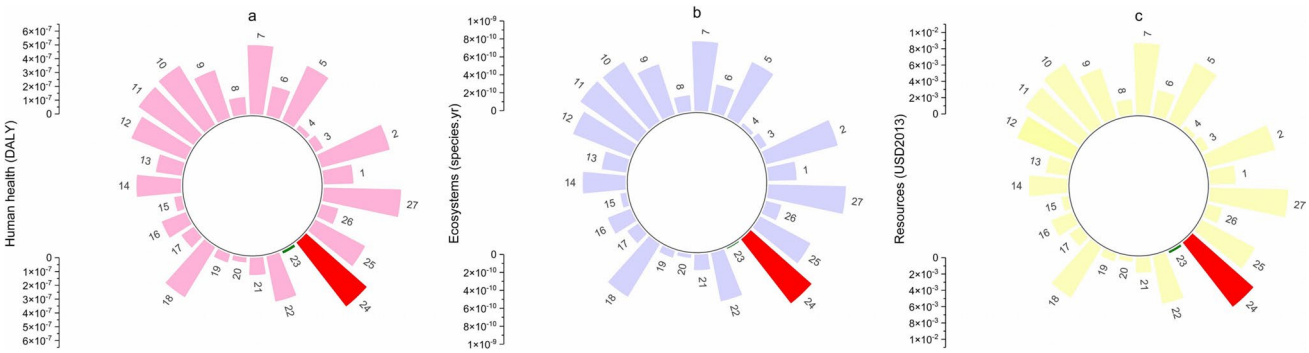

Fig. 5 Environmental damages of TC removal from water under different EC operational conditions: **a** human health damage (DALY), **b** ecosystem damage (species·yr), and **c** resource damage (USD2013) per FU

Scanning electron microscopy analysis

To further examine the morphological changes of the electrodes before and after EC treatment, Scanning Electron Microscopy (SEM) was employed. In this study, SEM analysis was conducted using the INCAx-act scanning electron microscope (Oxford Instruments, UK). The objective was to compare the surface condition of the electrodes before treatment, when the surface is expected to be relatively smooth and free of major deposits, with that after treatment, when electrochemical reactions typically lead to the formation of flocs, oxide layers, and surface irregularities. Such analysis provides valuable insight into electrode consumption, fouling, and pollutant removal mechanisms during EC.

The comparative SEM micrographs (Fig. 4) clearly illustrate the transformation of the electrode surfaces. Before treatment (Fig. 4a), the aluminum surface appeared relatively smooth and uniform, with no significant cracks, pits, or deposits, confirming a clean state suitable for electrochemical reactions. After treatment (Fig. 4b), the surface exhibited pronounced roughness, irregularities, and visible deposits, which are attributed to the formation of aluminum hydroxide flocs and oxide layers. Localized pitting and erosion marks were also observed, indicating active anodic dissolution during the process. This contrast demonstrates the dual role of electrodes: initially providing a stable surface for coagulant generation and subsequently undergoing fouling and structural degradation due to floc accumulation and material consumption.

Environmental assessment results

Figure 5a illustrates the human health damage category, expressed as Disability-Adjusted Life Years (DALY), associated with TC removal under various EC operational conditions. The results reveal a pronounced dependence of DALY on key process parameters, including pH, current intensity, electrode spacing, and treatment time. Across the 27 experimental runs, DALY values ranged from 1.787×10^{-8}/FU (Run 23) to 5.875×10^{-7}/FU (Run 24), indicating that the choice of operational conditions can result in more than a 30-fold variation in the potential human health damage category. Run 24 shows no significant improvement in TC removal compared to Run 23 (Fig. 2); therefore, the added acid did not achieve any considerable enhancement in removal efficiency; it only increased the environmental burden. Run 23, conducted at neutral pH (7) with low current intensity (10 mA), moderate electrode spacing (10 mm), and short treatment time (5 min), exhibited the lowest DALY per FU, reflecting minimal damage to human health. This outcome is attributed to several factors: the absence of chemical additives for pH adjustment, reduced energy consumption due to optimized electrical conditions, and effective pollutant removal without unnecessary extension of treatment time. Notably, although TC removal in this run was lower than in base-treated or high-current runs, it demonstrates a favorable balance between treatment efficiency and health risks. In contrast, Run 24, characterized by acidic pH (3), higher current intensity (20 mA), the same electrode spacing, and extended treatment time (30 min), achieved higher TC removal than Run 23 but resulted in the highest DALY per FU. This highlights a clear trade-off between pollutant removal efficiency and human health impacts, where operational intensification (chemical adjustment and longer treatment) enhances removal performance but substantially increases environmental burden.

Figure 5b also shows the damage to ecosystems, expressed in species.yr, resulting from TC removal under different EC operational conditions. Ecosystem damage ranged from 8.602×10^{-12} species.yr/FU (Run 23) to 9.056×10^{-10} species.yr/FU (Run 24), indicating that operational parameters can produce more than a 100-fold variation in potential damage to ecosystems. Similar to human health risk, Run 23, with neutral pH, low current, moderate electrode spacing, and short treatment time, resulted in the lowest ecosystem damage, reflecting minimal chemical

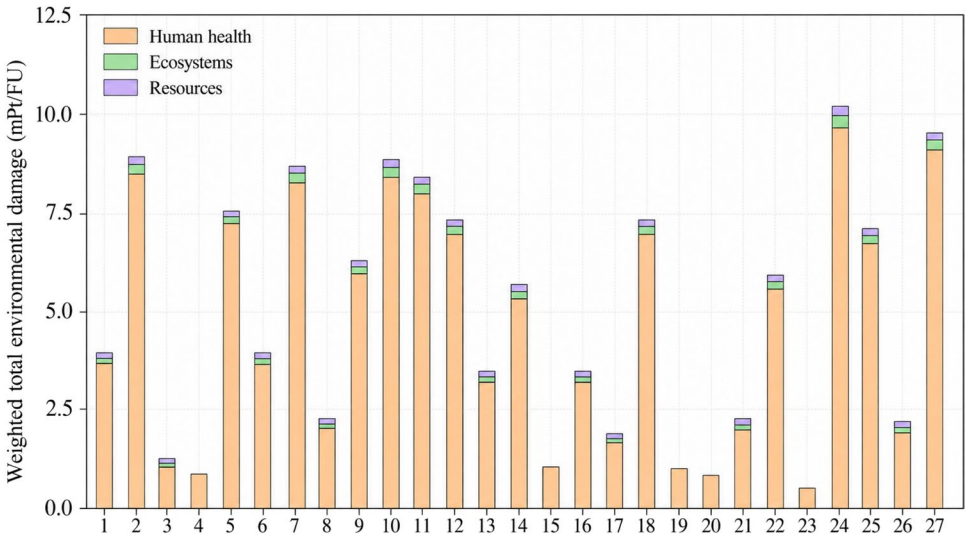

Fig. 6 Weighted total environmental damage of TC removal from water under different EC operational scenarios per FU

and energy inputs. In contrast, Run 24, with acidic pH, higher current, and long treatment time, caused the highest ecosystem damage, despite achieving higher TC removal. These results highlight a clear trade-off between treatment efficiency and ecological sustainability. Runs conducted under alkaline (base-adjusted) conditions demonstrated higher TC removal, indicating that increasing pH can enhance pollutant elimination. However, this improvement in removal efficiency did not translate into lower environmental impacts. The ecosystem damage in these runs was generally more serious than in neutral pH scenarios, due to the additional chemical inputs required for pH adjustment, higher electrical energy consumption, and, in some cases, longer treatment times, all of which cumulatively increase damage to ecosystems. Moreover, Fig. 5c shows the resource damage category for TC removal from water under different EC conditions. Run 23 caused the lowest resource damage of 0.00026 USD2013 per FU, while Run 24 had the highest at 0.00998 USD2013 per FU, nearly 38 times higher.

As shown in Fig. 6, weighted total environmental damage was also calculated to integrate human health, ecosystem, and resource impacts into a single score, providing a comprehensive assessment of the overall environmental burden of TC removal from water under different EC operational scenarios. Across all scenarios, weighted total environmental damage ranged from the lowest (Run 23, about 0.3 mPt/FU) to the highest (Run 24, about 10 mPt/FU), showing a more than 30-fold difference. In all cases, the human health damage category was the dominant contributor, followed by ecosystems and resources. Notably, based on the RSM model (Fig. 2), acidic pH conditions cannot achieve high TC removal efficiency. Run 24 (pH 3, 20 mA, 30 min) shows no significant improvement in TC removal compared to Run 23. Thus, the added acid failed to enhance removal efficiency and only increased the environmental burden, making Run 24 a clear lose-lose scenario. In contrast, Run 23 achieves a win–win balance with adequate removal and minimal environmental impact due to the absence of acid or base consumption.

Generally, the results show that improving TC removal was often accompanied by higher environmental damage, mainly because more intensive operating conditions required greater chemical addition and energy input. In contrast, moderate operating conditions provided a better sustainability profile by reducing the weighted total damage across all impact categories, although they resulted in a slightly lower TC removal efficiency. These findings are directly linked to the RSM analysis, as the operating parameters investigated through RSM—including pH, current intensity, inter-electrode distance, and electrolysis time—were incorporated into the LCA-based environmental assessment. This integration enables the identification of EC operating conditions that achieve a favourable balance between TC removal efficiency and environmental impact, thereby demonstrating the practical value of coupling RSM with LCA.

The RSM surface plots illustrating the combined effects of the principal EC operating parameters on the weighted total environmental damage associated with TC removal are presented in Fig. 7. These plots provide a holistic view of how pH, current intensity, electrode spacing, and treatment time interact to influence overall environmental burden. The

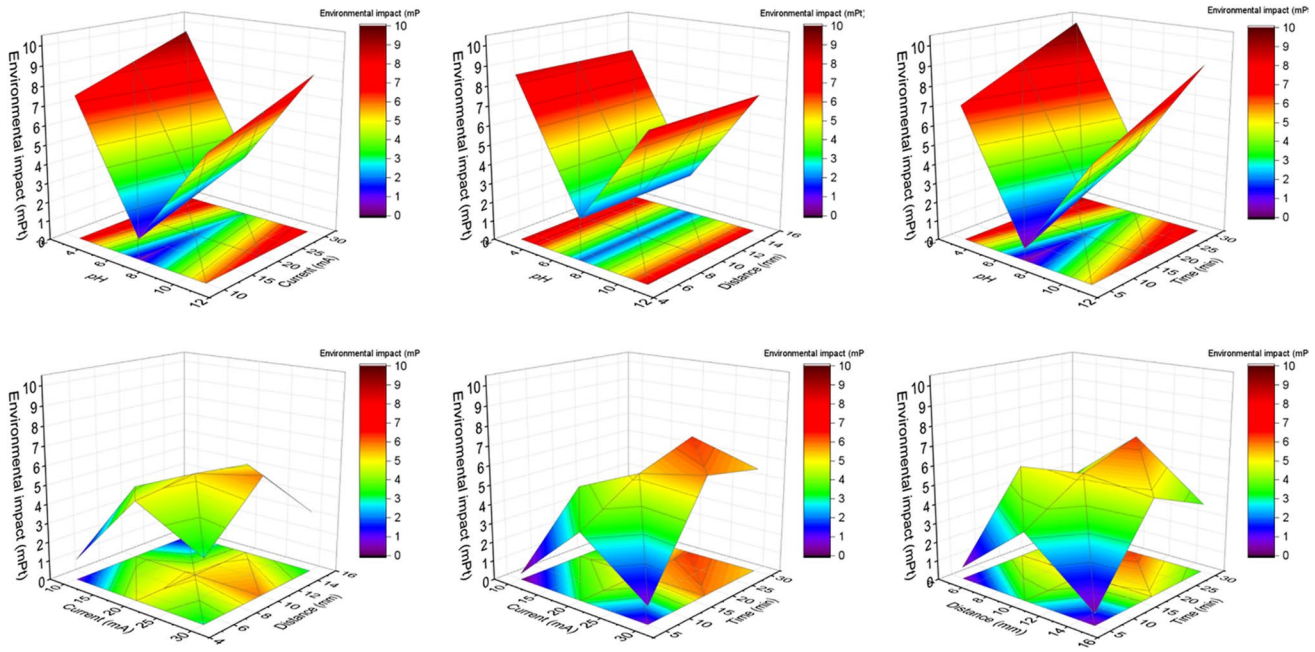

Fig. 7 Response surface plots of the influence of key EC operational parameters on weighted total environmental damage during TC removal from water per FU

surfaces reveal that extreme pH conditions, either strongly acidic or strongly alkaline, consistently amplify environmental impacts, while near-neutral pH mitigates them. Higher current intensities are associated with increased damage, primarily due to elevated energy consumption. Among the investigated variables, pH exerted the strongest influence on the weighted environmental damage. However, the relationship was not simply characterised by increasing damage with increasing pH; rather, the lowest impacts occurred near neutral pH, while deviations toward either acidic or alkaline conditions increased the environmental burden. Current and distance also have considerable effects, but their impact is less pronounced compared to pH rate. Electrolysis time showed the weakest individual influence, although it still contributed to changes in environmental performance, particularly when combined with higher current intensity. The observed interaction effects confirm that the environmental influence of each parameter depends on the levels of the other variables, reinforcing the need for multivariable optimization rather than evaluation of individual parameters in isolation.

The response surfaces point to an operational trade-off region where near-neutral pH, low-to-moderate current intensity, intermediate electrode spacing, and controlled electrolysis time minimized the weighted total environmental damage while still maintaining effective TC removal. This integrative visualization underscores the trade-offs inherent in EC treatment; enhancing pollutant removal without consideration of operational intensity can substantially increase environmental impacts. By linking these findings with RSM optimization, Fig. 7 provides a practical roadmap for selecting sustainable EC conditions, enabling a balanced approach that maximizes treatment efficiency while minimizing environmental burdens.

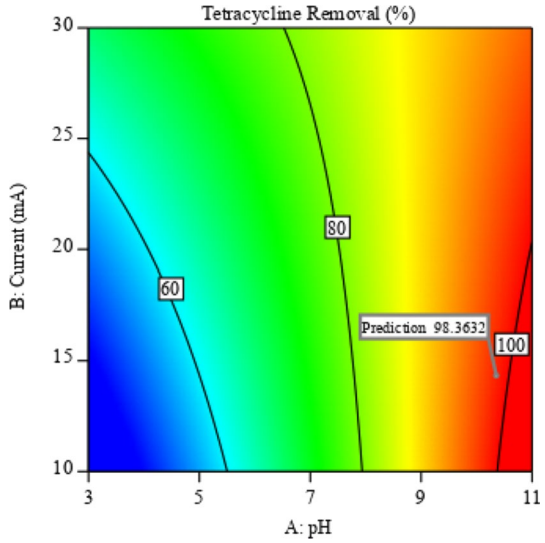

Fig. 9 Numerical optimization of the EC process using the desirability function approach for maximum TC removal under the optimum operating conditions predicted by the developed RSM model

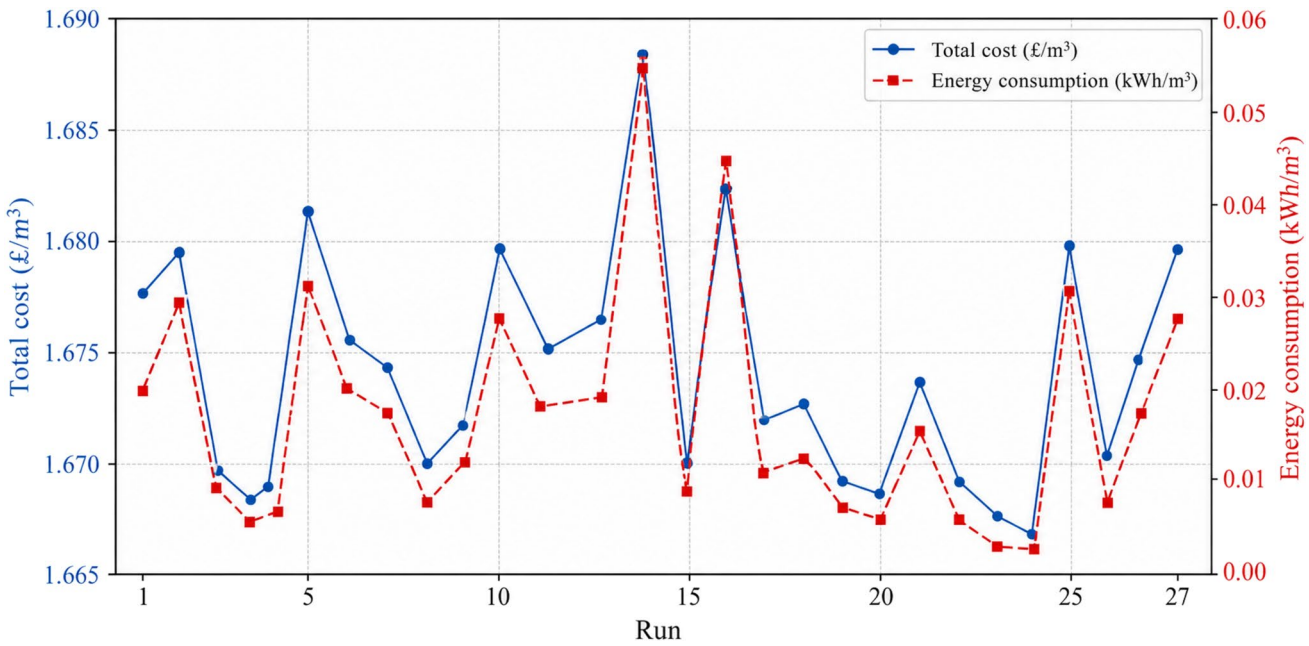

Fig. 8 Comparison of energy consumption (right axis) and total process cost (left axis) across 27 electrocoagulation runs for the removal of TC from aqueous solutions

Operation cost and optimization results

Figure 8 presents the relationship between energy consumption and total process cost for 27 experimental runs of EC treating TC solutions. The estimated energy requirement ranged from approximately 0.002 to 0.053 kWh/m^3, depending on current intensity, electrode spacing, and reaction time. In parallel, the total operating cost varied between £1.67 and £1.69 per cubic meter, with the chemical cost of NaCl (≈ £1.67/m^3) constituting the largest share. Electrode consumption contributed only a minor fraction (< £0.01/m^3), while energy costs showed modest variability (from < £0.001/m^3 under low current/time settings up to ~ £0.013/m^3 under more demanding conditions). These results highlight that, although the supporting electrolyte dominates the cost structure, operational parameters such as current density and electrolysis duration primarily govern the energy burden. Consequently, fine-tuning these parameters is essential to maintain pollutant removal efficiency while keeping energy demand and costs within a practical range.

After model development and statistical evaluation, numerical optimization was performed using the desirability function approach to determine the optimum EC operating conditions for maximum TC removal efficiency. In the optimization procedure, the response goal for TC removal was set to maximize, while pH, current intensity, inter-electrode distance, and electrolysis time were maintained within the experimental ranges investigated. As shown in Fig. 9, the developed quadratic model predicted the optimum operating region at alkaline pH, with pH 10.35, current intensity of 14.33 mA, inter-electrode distance of 14.52 mm, and electrolysis time of 10.21 min, resulting in a predicted TC removal efficiency of 98.36%. To verify the adequacy and predictive capability of the developed model, additional validation experiments were conducted under the optimized conditions obtained from the numerical optimization step. The experimental TC removal efficiency achieved under these conditions was 97.4%, which showed good agreement with the predicted value, with a relative deviation of 1%. This close agreement confirms the validity, reliability, and applicability of the developed RSM model for predicting and optimizing TC removal by the EC process.

Conclusion

This study demonstrated that aluminium-electrode electrocoagulation can effectively remove TC from aqueous solutions when the operating conditions are properly optimized. The BBD-RSM model showed that pH and electrolysis time were the dominant factors controlling TC removal, while inter-electrode distance had the weakest individual effect. Although maximum removal was achieved under more intensive alkaline/high-current conditions, the integrated RSM-LCA results showed that the technically highest removal condition was not necessarily the most sustainable option. The most favourable trade-off was obtained under near-neutral and moderate operating conditions, particularly at pH 7, low-to-moderate current intensity, 10 mm inter-electrode distance, and short electrolysis time, where TC removal remained high while the weighted environmental damage was minimized at approximately 0.3 mPt/FU. This confirms that EC optimization should not be based on removal efficiency alone, since operational intensification can increase chemical demand, energy use, and life-cycle impacts without proportional treatment benefits.

The cost analysis showed that NaCl addition was the dominant contributor to the estimated operating cost, exceeding the contributions of electricity and aluminium electrode consumption. Therefore, reducing the required dose of the supporting electrolyte, improving the conductivity of the influent through process integration, or evaluating alternative electrolytes should be prioritized to improve the economic feasibility of the process. Despite these promising results, the study has limitations. The experiments were conducted using synthetic TC-contaminated water at laboratory scale, and the effects of real water matrices, competing ions, natural organic matter, and variable conductivity were not assessed. In addition, sludge generation, sludge characterization, and end-of-life sludge handling were outside the system boundary. Future work should therefore validate the optimized EC conditions using real pharmaceutical wastewater or surface water, evaluate sludge management options, and test the process under pilot-scale continuous-flow conditions to better assess its technical feasibility, environmental performance, and potential for practical implementation.

Author contributions Sayedali Mirkhalafi: Methodology, Conceptualization, Data curation, Writing—original draft, Writing—review & editing, Visualization, Validation. Mohammadali Kiehbadroudinezhad: Software, Formal analysis, Writing—review & editing. Homa Hosseinzadeh-Bandbafha: Software, Formal analysis, Writing—review & editing. Milad Mousazadehgavan: Software, Formal analysis, Investigation, Methodology, Writing—review & editing. Khalid S. Hashim: Supervision, Project administration, Writing—review & editing.

Funding The authors declare that no funds were received during the preparation of this manuscript.

Declarations

Conflict of interest The authors declare no competing interests.

References

Ahangarnokolaei MA, Attarian P, Ayati B, Ganjidoust H, Rizzo L (2021) Life cycle assessment of sequential and simultaneous combination of electrocoagulation and ozonation for textile wastewater treatment. J Environ Chem Eng 9:106251

Ait Ouaissa Y, Chabani M, Amrane A, Bensmaili A (2014) Removal of tetracycline by electrocoagulation: kinetic and isotherm modeling through adsorption. J Environ Chem Eng 2:177–184

Al-Hashimi O, Hashim K, Loffill E, Nakouti I, Faisal AAH, Čebašek TM (2022) Kinetic and equilibrium isotherm studies for the removal of tetracycline from aqueous solution using engineered sand modified with calcium ferric oxides. Environments (Basel) 10:7

Al-Hashimi O, Hashim K, Loffill E, Nakouti I, Faisal AAH, Čebašek TM (2023) Eco-friendly remediation of tetracycline antibiotic from polluted water using waste-derived surface re-engineered silica sand. Sci Rep 13:13148

Al-Kilani MR, Bani-Melhem K (2025) The performance of electrocoagulation process for decolorization and COD removal of highly colored real grey water under variable operating conditions. Desalin Water Treat 321:100924

Almukdad A, Hawari AH, Hafiz M (2021) An enhanced electrocoagulation process for the removal of Fe and Mn from municipal wastewater using dielectrophoresis (DEP). Water 13:485

Al-Qodah Z, AL-Rajabi MM, Al Amayreh HH, Assirey E, Bani-Melhem K, Al-Shannag M (2025) Performance of continuous electrocoagulation processes (CEPs) as an efficient approach for the treatment of industrial organic pollutants: a comprehensive review. Water. https://doi.org/10.3390/w17152351

Ansari K, Shrikhande A, Malik MA, Alahmadi AA, Alwetaishi M, Alzaed AN, Elbeltagi A (2022) Optimization and operational analysis of domestic greywater treatment by electrocoagulation filtration using response surface methodology. Sustainability 14:15230

Antos J, Piosik M, Ginter-Kramarczyk D, Zembrzuska J, Kruszelnicka I (2024) Tetracyclines contamination in European aquatic environments: a comprehensive review of occurrence, fate, and removal techniques. Chemosphere 353:141519

Anuf AR, Ramaraj K, Sivasankarapillai VS, Dhanusuraman R, Maran JP, Rajeshkumar G, Rahdar A, Díez-Pascua AM (2022) Optimization of electrocoagulation process for treatment of rice mill effluent using response surface methodology. J Water Process Eng 49:103074

Atashzaban Z, Seidmohammadi A, Nematollahi D, Azarian G. Heidary SO, Rahmani AR (2016) The efficiency of electrocoagulation and electroflotation processes for removal of polyvinyl acetate from synthetic effluent.

Barbhuiya S, Das BB (2023) Life cycle assessment of construction materials: methodologies, applications and future directions for sustainable decision-making. Case Stud. Constr. Mater. 19:e02326

Bazrafshan E, Moein H, Kord Mostafapour F, Nakhaie S (2013) Application of electrocoagulation process for dairy wastewater treatment. J Chem 2013:640139

Boinpally S, Kolla A, Kainthola J, Kodali R, Vemuri J (2023) A state-of-the-art review of the electrocoagulation technology for wastewater treatment. Water Cycle 4:26–36

Dong H, Chi W, Gao A, Xie T, Gao B (2021) Electrochemical degradation of tetracycline using a Ti/Ta_2O_5-IrO_2 anode: performance, kinetics, and degradation mechanism. Materials (Basel) 14:4325

Ensano BMB, Borea L, Naddeo V, Belgiorno V, De Luna MDG, Ballesteros FC Jr (2017) Removal of pharmaceuticals from wastewater by intermittent electrocoagulation. Water 9:85

Felis E, Kalka J, Sochacki A, Kowalska K, Bajkacz S, Harnisz M, Korzeniewska E (2020) Antimicrobial pharmaceuticals in the aquatic environment-occurrence and environmental implications. Eur J Pharmacol 866:172813

Finnveden G, Hauschild MZ, Ekvall T, Guinée J, Heijungs R, Hellweg S, Koehler A, Pennington D, Suh S (2009) Recent developments in life cycle assessment. J Environ Manage 91:1–21

Gadekar MR, Ahammed MM (2019) Modelling dye removal by adsorption onto water treatment residuals using combined response surface methodology-artificial neural network approach. J Environ Manage 231:241–248

Hassaan MA, Elkatory MR, El-Nemr MA, Ragab S, Mohamed BA, El Nemr A (2023) Box-Behnken design and life cycle assessment for nickel oxide nanoparticles application in biomethane production. Chem Eng J 474:145924

Hawari AH, Alkhatib AM, Hafiz MA, Das P (2020) A novel electrocoagulation electrode configuration for the removal of total organic carbon from primary treated municipal wastewater. Environ Sci Pollut Res 27:23888–23898

He Y, Hosseinzadeh-Bandbafha H, Kiehbadroudinezhad M, Peng W, Tabatabaei M, Aghbashlo M (2023) Environmental footprint analysis of gold recycling from electronic waste: A comparative life cycle analysis. J Clean Prod 20:139675

Igwegbe CA, Obi CC, Onyechi CC, Davoud B, Owiec BA, Onukwuli OD (2024) Integration of experimental and intelligent modeling for optimizing iron electrocoagulation-flocculation recovery of aquafarm effluent Desalin. Water Treat 320:100832

ISO (2006a) 14040 international standard. Environmental management–life cycle assessment–principles and framework, international organisation for standardization, Geneva, Switzerland. [WWW Document]. URL https://www.iso.org/standard/37456.html

ISO (2006b) 14044 international standard. Environmental management–life cycle assessment–requirements and guidelines, international organisation for standardization, Geneva, Switzerland. [WWW Document]. URL https://www.iso.org/standard/38498.html

Janpoor F, Torabian A, Khatibikamal V (2011) Treatment of laundry waste-water by electrocoagulation. J Chem Technol Biotechnol 86:1113–1120

Jensen WA (2017) Response surface methodology: process and product optimization using designed experiments 4th edition. J Qual Technol 49:186–188

Kiehbadroudinezhad M, Hosseinzadeh-Bandbafha H, Karimi K, Madadi M, Chisti Y, Peng W, Liu D, Tabatabaei M, Aghbashlo M (2023) Production of chemicals and utilities in-house improves the environmental sustainability of phytoplankton-based biorefinery. Sci Total Environ 899:165751

Kothari MS, Shah KA (2020) Electrochemical oxidation for decolorization of Rhodamine-B dye using mixed metal oxide electrode: modeling and optimization. Water Sci Technol 81:720–731

Kothari MS, Vegad KG, Shah KA, Hassan AA (2022) An artificial neural network combined with response surface methodology approach for modelling and optimization of the electro-coagulation for cationic dye. Heliyon. https://doi.org/10.1016/j.heliyon.2022.e08749

Kumari M, Gupta SK (2019) Response surface methodological (RSM) approach for optimizing the removal of trihalomethanes (THMs) and its precursor's by surfactant modified magnetic nanoadsorbents (sMNP) - an endeavor to diminish probable cancer risk. Sci Rep 9:18339

Liu M, Liu Y, Bao D, Zhu G, Yang G, Geng J, Li H (2017) Effective removal of tetracycline antibiotics from water using hybrid carbon membranes. Sci Rep 7:43717

Loya-González D, Loredo-Cancino M, Soto-Regalado E, Rivas-García P, de Jesús Cerino-Córdova F, García-Reyes RB, Bustos-Martínez D, Estrada-Baltazar A (2019) Optimal activated carbon production from corn pericarp: a life cycle assessment approach. J Clean Prod 219:316–325

Lu J, Xu K, Li W, Hao D, Qiao L (2018) Removal of tetracycline antibiotics from aqueous solutions using easily regenerable pumice: batch and column study. Water Qual Res J 53:143–155

Lu J, Zhang W, Zhang X, Si G, Zhang P, Li B, Su R, Gao X (2021) Efficient removal of Tetracycline-Cu complexes from water by electrocoagulation technology. J Clean Prod 289:125729

Mirkhalafi S, Hashim KS, Al-Hashimi O, Majdi A (2024) Hybrid electrocoagulation–adsorption process for Montelukast sodium removal from water. Clean Technol 6:1537–1564

Mirkhalafi S, Mohammadnezhad B, Mousazadehgavan M, Kiehbadroudinezhad M, Altaee A, Hosseinzadeh-Bandbafha H, Hashim K (2025) Technical and environmental sustainability of pharmaceutical wastewater treatment using Ce-NaY zeolite-modified polyethersulfone (PES) membranes: a life cycle assessment approach. ACS EST Water. https://doi.org/10.1021/acsestwater.5c00162

Mousazadeh M, Naghdali Z, Al-Qodah Z, Alizadeh SM, Niaragh EK, Malekmohammadi S, Nidheesh PV, Roberts EPL, Sillanpää M, Emamjomeh MM (2021) A systematic diagnosis of state of the art in the use of electrocoagulation as a sustainable technology for pollutant treatment: An updated review. Sustain Energy Technol Assessments 47:101353

Naje AS, Chelliapan S, Zakaria Z, Abbas SA (2015) Treatment performance of textile wastewater using electrocoagulation (EC) process under combined electrical connection of electrodes. Int J Electrochem Sci 10:5924–5941

Nariyan E, Aghababaei A, Sillanpää M (2017) Removal of pharmaceutical from water with an electrocoagulation process; effect of various parameters and studies of isotherm and kinetic. Sep Purif Technol 188:266–281

Olya ME, Pirkarami A (2013) Electrocoagulation for the removal of phenol and aldehyde contaminants from resin effluent. Water Sci Technol 68:1940–1949

Patel P, Gupta S, Mondal P (2023) Life cycle assessment (LCA) of greywater treatment using $ZnCl_2$ impregnated activated carbon and electrocoagulation processes: a comparative study. Ind Eng Chem Res 62:3259–3270

Ribeiro JP, Sarinho L, Nunes MI (2024) Application of life cycle assessment to Fenton processes in wastewater treatment–A review. J Water Process Eng 57:104692

Rosenbaum RK, Hauschild MZ, Boulay A-M, Fantke P, Laurent A, Núñez M, Vieira M (2018) Life cycle impact assessment. Life Cycle Assessment. Springer, pp 167–270

Sedaghat O, Bahramifar N, Nowrouzi M, Younesi H (2025) Life cycle assessment of industrial wastewater treatment: evaluating the environmental impact of electrocoagulation technologies. J Water Process Eng 71:107257

Shakeri E, Mousazadeh M, Ahmadpari H, Kabdaşlı I, k, Jamali, H.A., Graça, N.S., Emamjomeh, M.M., (2021) Electrocoagulation-flotation treatment followed by sedimentation of carpet cleaning wastewater: optimization of key operating parameters via RSM-CCD. Desalin Water Treat 227:163–176

Shang X, Zhang L, Chang J, Jiao Y, Gong B, Yang J, Zhong R (2024) Mix proportion design and life cycle assessment of ultra-high-performance lightweight concrete with hollow microspheres. Constr Build Mater 449:138462

Sheikh S, Naghizadeh-Dehno O, Mirkhalafi S, Ghashang M (2024) Magnetic heterogenization of supramolecular carbohydrates for the efficient adsorption of heavy metals removal from wastewater. Inorg Chem Commun 168:112835

Silva GF, Camargo FL, Ferreira ALO (2011) Application of response surface methodology for optimization of biodiesel production by transesterification of soybean oil with ethanol. Fuel Process Technol 92:407–413

Tegladza ID, Xu Q, Xu K, Lv G, Lu J (2021) Electrocoagulation processes: a general review about role of electro-generated flocs in pollutant removal. Process Saf Environ Prot 146:169–189

Wang S, Li F, Sadhukhan J, Xuan J, Mao X, Xing L, Zhao X, Wang X (2024) Revealing the best solution simultaneously for environmental and economic performance using response surface methodology under the perspective of life cycle: a case study of sludge dewatering by the Fenton process. J Clean Prod 434:139846

Zaied BK, Rashid M, Nasrullah M, Zularisam AW, Pant D, Singh L (2020) A comprehensive review on contaminants removal from pharmaceutical wastewater by electrocoagulation process. Sci Total Environ 726:138095

Zhang Z, Sun K, Gao B, Zhang G, Liu X, Zhao Y (2011) Adsorption of tetracycline on soil and sediment: effects of pH and the presence of Cu (II). J Hazard Mater 190:856–862

Zhang H, Bian J, Yang C, Hu Z, Liu F, Zhang C (2022) Removal of tetracycline from livestock wastewater by positive single pulse current electrocoagulation: mechanism, toxicity assessment and cost evaluation. Sci Total Environ 810:151955

Authors and Affiliations

S. Mirkhalafi[1,2] · M. Kiehbadroudinezhad[3] · H. Hosseinzadeh-Bandbafha[4] · M. Mousazadehgavan[1] · K. S. Hashim[1,5,6]

✉ M. Mousazadehgavan
m.mousazadehgavan@2024.ljmu.ac.uk

[1] Faculty of Engineering and Technology, School of Civil Engineering and Built Environment, Liverpool John Moores University (LJMU), Liverpool L3 3AF, UK

[2] Water Research Center, School of Biological Sciences, Adelaide University, Adelaide, South Australia 5005, Australia

[3] Circular Process Engineering Laboratory, Department of Process Engineering and Applied Science, Dalhousie University, Halifax, NS, Canada

[4] Environmental Research and Sustainability Division, Malus Ecolife Inc., Halifax, NS, Canada

[5] University of Babylon, Hillah, Iraq

[6] Research Centre for Sustainable Process Technology (CESPRO), Faculty of Engineering and Built Environment, Universiti Kebangsaan Malaysia, Bangi, Malaysia